An Uncontrolled Toy That Can Walk But Cannot Stand Still

Michael J. Coleman and Andy Ruina
Department of Theoretical and Applied Mechanics
Cornell University, Ithaca, NY 14853-7501 USA
Submitted to Physical Review Letters, June 14, 1997
(revised November 18, 1997)

physics/9711006 v3 18 Nov 1997

We built a simple two-leg toy that can walk stably with no control system. It walks downhill powered only by gravity. It seems to be the first McGeer-like passive-dynamic walker that is statically unstable in all standing positions, yet is stable in motion. It is one of few known mechanical devices that are stable near a statically unstable configuration but do not depend on spinning parts. Its design is loosely based on simulations which do not predict its observed stability. Its motion highlights the possible role of uncontrolled nonholonomic mechanics in balance.

Introduction. Human walking on level ground involves dynamic balance which, if viewed in a course–grained way, is presumably asymptotically stable. This observed stability of walking must depend on some combination of neurological control and mechanical features. The common view is that neuro-muscular control is responsible for this balance. To what extent is neuro-muscular coordination of animal locomotion, say human walking, really necessary? The bold proposal of McGeer [1,2,3,4,5,6] is that much of the stabilization of walking might be understood without control.

The possibility that asymptotically stable balance can be achieved without control is somewhat unintuitive since top-heavy upright things tend to fall down when standing still or, more generally, since dynamical systems often run away from potential energy maxima. Two mechanics issues that bear on such stability considerations are that: 1) Hamiltonian (conservative and holonomic) dynamical systems cannot have asymptotic stability, and 2) conservative *non*holonomic systems can have asymptotically (exponentially) stable steady motions in some variables while at most mildly unstable in the others, as recalled in Zenkov, *et al.* [7].

Since before the clever patent of Fallis in 1888 [8] (the oldest reference we have), there have been two and four leg passive-dynamic walking toys that either walk downhill or that walk on level ground when pulled by a string. All such toys that we know about are statically stable when they are not walking. While their motion is engaging to watch, their dynamic stability is perhaps not so great a surprise.

McGeer's passive-dynamic walkers. Inspired by a double pendulum simulation of swinging legs [9] and by simple walking toys, McGeer successfully sought and found two-dimensional, straight-legged and kneed walking model designs that displayed graceful, stable, human-like walking on a range of shallow slopes with no actuation (besides gravity) and no control. McGeer termed the motions of these machines *passive-dynamic* walking. All of McGeer's successful designs, as well as those of his imitators thus far [10,11,12], have been more-or-less constrained against falling over sideways so that their dynamic balance is fore-aft only. These machines cannot stand stably upright except when their legs are spread fore and aft. The dynamic stability of these devices could be dependent on the static stability of this spread-leg configuration which is visited momentarily during walking.

While human walking motion is mostly in the sagittal (fore-aft and vertical) plane, the stability of out-of-plane (sideways) motions is an issue important to a more complete understanding of three-dimensional walking. McGeer's [4] numerical 3-D studies only led to unstable periodic motions. Fowble and Kuo [13] numerically simulated a passive-dynamic 3D model of walking but also did not find stable passive motions.

Our recent investigations of walking balance have been based on attempts to design mechanisms that vaguely mimic human geometry and walk without control. This paper describes one such primitive design (first reported in [14]) which extends to three dimensions, at least experimentally, the remarkable two-dimensional walking mechanisms of McGeer.

Spinning parts and nonholonomic constraints. Humans are notably lacking in gyros, flywheels or other spinning parts. Things with spinning parts, like tops and gyros, are well known to be capable of balancing near a potential energy maximum. The common model of an energy conserving point-contact gyro, however, does not have asymptotic stability since it is Hamiltonian. Adding a rounded tip to the top, with nonholonomic rolling contact, is not stabilizing. A spinning top with dissipation, however, can be asymptotically stable in a transient sense in that, over a limited time until the spinning rate has slowed too much, vertical motion is approached exponentially. The observed asymptotic stability of rolling coins and the like also depends on dissipation.

We know of only a few uncontrolled three-dimensional devices that can have asymptotically stable steady motions at or near a potential energy maximum, without depending on fast spinning parts. These devices are all nonholonomically-constrained and conservative: (1) a no-hands bicycle with massless wheels (say skates) and a special mass distribution [15,16]; (2) closely related to the bicycle is a rolling disk with eccentric masses that bank and steer but do not pitch with the disk [16,11]; (3) a no-hands tricycle (where gyroscopic terms from the spinning wheels are not relevant for balance because of the three point support) with a mildly soft de-centering (negative spring constant) spring on the steering [17,18]; (4) a rigid rider attached appropriately to a moving skate-board [19]; and (5) a statically unstable boat with an ideal keel, acting as a nonholonomic constraint, that is steered by the boat lean similarly to how a bicycle front wheel is steered by bike lean [20]. Certain gliding aircraft might also be considered as an example, but the definition of a potential energy maximum is less clear for planes since there is no well

defined reference for measuring potential energy.

All of these devices differ from walking mechanisms in that they are constrained against fore-aft tipping (the walking devices have fore-aft dynamics), they conserve energy (the walkers lose energy at joint and foot impacts and use up gravitational potential energy), and they are nonholonomically constrained (most of the walkers are well modeled as piecewise holonomic).

Intermittent contact and nonholonomicity. Mechanical systems that are asymptotically stable must be non-Hamiltonian. Two mechanisms for losing the Hamiltonian structure of governing equations are dissipation and nonholonomic constraints. The primary examples of nonholonomic constraint are rolling contact and skate-like sliding contact. For these two smooth constraints, and other less physical nonholonomic constraints, the set of allowed differential motions is not integrable. That is, the constraints are not equivalent to a restriction of the space of admissible configurations. For smooth nonholonomic systems, the dimension of the configuration space accessible to the system is greater than the dimension of the velocity space allowed by the constraints.

An intermittent non-slipping contact constraint can also cause the dimension of the accessible configuration space to be greater than the dimension of the accessible velocity space. As suggested by one simple example [21], this discrete nonholonomicity may account for exponential stability of some systems. The walking models we study are all nonholonomic in this intermittent sense (and also in the conventional sense if they have rounded feet). They can, for example, translate forwards by walking although the contact constraint does not allow forward sliding.

Dynamical modeling. Fig. 1 shows a 3D model which probably captures the essential geometric and mass-distribution features of the physical model presented here. The device, at least at the level of approximation which we believe is appropriate, is a pair of symmetric rigid bodies (leg 1 = stance leg, leg 2 = swing leg) that have mass m, symmetrically located (in the rest state) centers of mass $G_{1,2}$, and mirror-symmetry related moment of inertia matrices with respect to the center of mass $\mathbf{I}_{1,2}$. The legs are connected by a frictionless hinge at the hip with center point H and orientation $\hat{\mathbf{n}}$ normal to the symmetry plane of the legs. Each of the two legs can make rolling and collisional contact with the ground (slope = α) with no contact couples. The gravitational acceleration is $\mathbf{g}$.

The (reduced) dynamical state of the model is determined by the orientations and angular velocities of the legs. The stance leg orientation is determined by standard Euler angles ψ, $\theta_{\rm st}$, ϕ for lean, pitch and steer. The configuration of the swing leg is described by the angle $\theta_{\rm sw}$. The absolute position of the walker on the plane does not enter into the governing equations. The instantaneous point of contact of the stance leg with the ground is C and the point of the impending contact is D. We assume ground collisions are without bounce or slip.

The unreduced accessible configuration space is six-dimensional (the above angles plus position on the slope) whereas at any instant in time the accessible velocity space is four-dimensional (the four dynamical state variables). Hence the overall nonholonomicity ($6 > 4$) of this system which is smooth and holonomic at all but instants of collision. The model is also dissipative due to kinetic energy loss at the collisions.

The model is well-posed since the governing equations for rigid bodies in hinged, rolling, and plastic-collisional contact are well established. The equations which govern the evolution of the state of the system $\mathbf{q} = \{\phi, \dot{\phi}, \psi, \dot{\psi}, \theta_{\rm st}, \dot{\theta}_{\rm st}, \theta_{\rm sw}, \dot{\theta}_{\rm sw}\}$ follow from angular momentum balance (or other equivalent principles). Between collisions, we have angular momentum balance for the whole system about the contact point C

$$\sum_{i=1,2} \mathbf{r}_{G_i/C} \times m\mathbf{g} = \sum_{i=1,2} \left[\mathbf{r}_{G_i/C} \times m\mathbf{a}_i + \boldsymbol{\omega}_i \times (\mathbf{I}_i\boldsymbol{\omega}_i) + \mathbf{I}_i\dot{\boldsymbol{\omega}}_i\right] \tag{1}$$

where $\mathbf{r}_{G_i/C} \equiv \mathbf{r}_{G_i} - \mathbf{r}_C$, the center of mass velocities and accelerations are $\mathbf{v}_{1,2}$ and $\mathbf{a}_{1,2}$, and the angular velocities are $\boldsymbol{\omega}_{1,2}$. Angular momentum balance for the swing leg about the hip axis $\hat{\mathbf{n}}$ is

$$\hat{\mathbf{n}} \cdot \left\{\mathbf{r}_{G_2/H} \times m\mathbf{g} = \mathbf{r}_{G_2/H} \times m\mathbf{a}_2 + \boldsymbol{\omega}_2 \times (\mathbf{I}_2\boldsymbol{\omega}_2) + \mathbf{I}_2\dot{\boldsymbol{\omega}}_2\right\} \tag{2}$$

The eight collisional jump conditions come from continuity of configuration through the collision, conservation of angular momentum of the system about the new contact point D,

$$\sum_{i=1,2} \mathbf{r}_{G_i/D} \times m\mathbf{v}_i + \mathbf{I}_i\boldsymbol{\omega}_i \Big|_- = \sum_{i=1,2} \mathbf{r}_{G_i/D} \times m\mathbf{v}_i + \mathbf{I}_i\boldsymbol{\omega}_i \Big|_+ \tag{3}$$

and conservation of angular momentum for the swing leg about the swing hinge axis

$$\hat{\mathbf{n}} \cdot \left\{\mathbf{r}_{G_1/H} \times m\mathbf{v}_1 + \mathbf{I}_1\boldsymbol{\omega}_1 \big|_- = \mathbf{r}_{G_2/H} \times m\mathbf{v}_2 + \mathbf{I}_2\boldsymbol{\omega}_2 \big|_+\right\} \tag{4}$$

where the respective sides are to be evaluated just before $(-)$ and after $(+)$ foot collision with the ground. The second jump condition Eqn. (4) is being applied to the same leg as it switches from stance (subscript 1) to swing (subscript 2). Both jump conditions, Eqns. (3) and (4) also assume no collisional impulse from the ground to the leg which is just leaving the ground.

The governing equations and jump conditions above are expressed in terms of positions, velocities, and accelerations, which are all complicated functions of the state variables. As a result, the governing equations are massive expressions (pages long). We assembled the kinematic expressions and governing differential equations using symbolic algebra software (MAPLE).

The no-slip rolling condition is that the velocity of the material point in contact at C is zero. The acceleration of this point, needed to calculate the accelerations of $G_{1,2}$, is given by $\boldsymbol{\omega}^* \cdot \mathbf{R}\boldsymbol{\omega}^*$ where $\boldsymbol{\omega}^*$ is the in-the-contact-plane part of the angular velocity and $\mathbf{R}$ is the inverse of the local surface curvature matrix. So far, we have only studied a simplification with point-contact feet ($r_1 = r_2 = 0$, $\mathbf{R}$ is the zero matrix) and no hip spacing ($w = 0$). In this case, when a foot is on the ground, the contact acts like a ball-and-socket joint and the only nonholonomy is that of intermittent contact.

In order to study the stability of such systems, following McGeer, we represent an entire gait cycle by a Poincaré map

$$\mathbf{f}(\mathbf{q}_k) = \mathbf{q}_{k+1} \tag{5}$$

from the state of the system $\mathbf{q}_k$ *just* after a foot collision to the state $\mathbf{q}_{k+1}$ *just* after the next collision of the same foot (two leg swings and two foot collisions per map iteration). We evaluate $\mathbf{f}$ using numerical integration of Eqns. (1) and (2) between collisions and applying the jump conditions Eqns. (3) and (4), at each foot collision. For this model, the map is seven-dimensional $(8-1)$, but we treat it as eight-dimensional for numerical convenience.

Fixed points of the return map $\mathbf{f}$ ($\mathbf{q}$ with $\mathbf{f}(\mathbf{q}) = \mathbf{q}$) correspond to periodic gait cycles (not necessarily stable). We find fixed points by numerical root finding on the function $\mathbf{f} - \mathbf{q}$, sometimes using fixed points from models with nearby parameter values to initialize searches.

We determine the stability of periodic motions by numerically calculating the eigenvalues of the linearization of the return map at the fixed points. If the magnitudes of some of the eigenvalues are less than one (with all others equal to one), then the fixed point is asymptotically stable in those variables. Because there are a family of limit cycles at different headings one eigenvalue is always one. Because we use eight instead of seven dimensions in our map, one eigenvalue is always zero.

To date, like McGeer [4] and Fowble and Kuo [13] who studied similar simulations, we have found only unstable periodic motions, though less unstable than theirs. A nearly stable case from our numerical studies has maximum eigenvalue modulus of about 1.15, one of exactly one, and the other six less than one. Fore-aft balance has already been achieved with two-dimensional walking models whose stable fixed points we use as starting points for the 3D analysis. Thus the eigenvector associated with the maximum eigenvalue corresponds to falling over sideways (i. e., is dominated by $\psi, \dot{\psi}$ component) as expected. The most stable mass distributions we have found do not have very human-like parameters; each leg has a center of mass closer to the foot than the hip, and laterally displaced at about 90% of the leg length.

In this almost-stable case, the walker's legs have a mass distribution corresponding roughly to laterally extended balance bars, like what might be used for walking on a tightrope. In the limit, as the lateral offset of the center of mass gets very large, the device approaches, for sideways balance, an inverted pendulum with large rotational inertia. The step periods remain bounded. Negligible falling acceleration can thus occur in one step and the modulus of the maximum eigenvalue of the linearized step–to–step map asymptotically approaches one, or apparent neutral stability, from *above*. Thus the closeness of the largest map eigenvalue modulus to one is not a complete measure of closeness to stability. However, when averaged over a step cycle, this model does fall more slowly than a corresponding inverted pendulum and the low eigenvalue is not just a result of slowed falling due to large rotary inertia.

The toy. As a non-working demonstration of the kinematics and mass distributions in our simulations, and not for walking experiments, we assembled a device similar to the one shown in Fig. 2. It has two straight legs, separated by simple hinges at the hips, laterally extending balance mass rods, and rounded feet. Playing, with no hopes of success, we placed the toy on a ramp. Surprisingly, it took a few serendipitous, if not very steady or stable, steps. After some non-quantifiable tinkering, we arrived at the functioning device shown.

Our physical model is constructed from a popular American child's construction toy, brass strips to round the feet bottoms, and various steel nuts for balance masses. The walking ramp has about a 4.5 degree slope and is narrow enough to avoid making contact with the balance masses as the walker rocks side-to-side. Another more complex assembly of similar toy parts (not described here) walks on a wide ramp.

Aside: construction details. The device is built using the Playskool® Tinkertoy® Construction System: Colossal Constructions™, 1991 set. One leg is made from a yellow spool, a light green rod, and a dark green hinge (plus '+' shaped) glued together. Then, we slid the legs onto a red rod (loose fit) which acts as an axle. The green hinges are separated and kept from sliding apart by three orange washers friction-fit to the red axle. The legs and red axle can rotate independently.

To support the side weights, we glued a yellow spool rigidly to the end of a red rod and inserted the other end into the side of a yellow foot with a friction fit to allow for rotational adjustment.

We assembled each balance mass from two stacked steel nuts held together between two washers by a nut and bolt. Each nut assembly has a mass of about 50 grams. Then, each balance mass assembly was located on the yellow spools at the end of the balance rods and held in place with vinyl electrical tape. The balance mass assembly is tilted behind the leg. As a result, the legs have low mass centers located laterally at a distance comparable to the leg length, above the center of curvature of the feet, and just behind the leg axes. The mass of the fully assembled walking device is about 120 grams, only 20 grams more than the two balance masses. When the toy is in its unstable-equilibrium standing position the nominally-vertical legs are approximately orthogonal to the ramp.

Because a yellow spool has holes located radially around its circumference to accept rods, a small flat section is on the bottom at the foot contact point. To ensure that the walker is statically unstable (cannot stand on the flat sections or in any other way), a small (0.50 cm wide) strip of thin (0.013 cm) brass shim stock material was fastened over the flat section contacting the floor so as to restore its curvature there.

Observed motion. Because the center of mass is above the center of curvature of the round feet, we cannot stably stand this device with parallel or with splayed legs. When placed aiming downhill on a ramp, tipped to one side, and released, the device rocks side-to-side and, coupled with swinging of the legs, takes tiny steps. When a foot hits the ground, it sticks and then rolls, until the swinging foot next collides with the ground. Except at the moment of foot collision, only one foot is in contact with the ground at any time. When the swinging foot collides with the ground, the trailing leg leaves the ground. The gait is more-or-less steady; after small disturbances the toy either falls or stumbles a few steps while returning to near-periodic gait. At a slope of 4.5 degrees, it takes a step about every 0.47 seconds and advances forward about 1.3 cm per step, where a step is measured from a foot

collision to the next collision of that same foot. The side-to-side tilt is about 4 degrees, there is no visible variation in ϕ during a step, but there is slight directional drift (one way or another) over many steps. The rounded metal strips at the feet bottom deform during foot collision in a way that may or may not be essential; we do not know.

Conclusions. We have constructed a device which can balance while walking but cannot stand in any configuration. Although our new machine does not have a very human-like mass distribution, it does highlight the possibility that uncontrolled dynamics may not just contribute to fore-aft walking balance, as indicated by previous McGeer models, but also to side-to-side balance. The mechanism joins a small collection of statically unstable devices which dynamically balance without any rapidly spinning parts.

Our too-simple mathematical/computational model does not explain this behavior. We do not yet know what key modeling features need be included to predict the observed dynamic stability. An open and possibly unanswerable question is whether the stability of this intermittently dissipative system can be explained, in part, by the fact that its piecewise holonomic constraints act somewhat like nonholonomic constraints.

Acknowledgments. Thanks to Les Schaffer, Saskya van Nouhuys, and Mariano Garcia for editorial comments.

[1] T. McGeer, in *Proc., IEEE International Conference on Robotics and Automation*, IEEE (IEEE, Piscataway, NJ, 1989), pp. 1592–7.
[2] T. McGeer, Intern. J. Robot. Res. **9**, 62 (1990).
[3] T. McGeer, in *Proc., 1990 IEEE International Conference on Robotics and Automation*, IEEE (IEEE, Los Alamitos, CA, 1990), pp. 1640–5.
[4] T. McGeer, in *Proc., Experimental Robotics II: The 2nd International Symposium*, edited by R. Chatila and G. Hirzinger (Springer–Verlag, Berlin, 1992), pp. 465–90.
[5] T. McGeer, in *Mechanics of Animal Locomotion*, Vol. 11 of *Advances in Comparative and Environmental Physiology*, edited by R. M. Alexander (Springer–Verlag, Berlin, 1992), Chap. Principles of Walking and Running.
[6] T. McGeer, J. theor. Biol. **163**, 277 (1993).
[7] D. Zenkov, A. Bloch, and J. Marsden, Technical report, University of Michigan (unpublished).
[8] G. T. Fallis, Walking Toy ('Improvement in Walking Toys'), U. S. Patent, No. 376,588, 1888.
[9] S. Mochon and T. McMahon, Math. Biosci. **52**, 241 (1980).
[10] M. Garcia, A. Chatterjee, A. Ruina, and M. J. Coleman, ASME J. Biomech. Eng. (1997), in press.
[11] M. J. Coleman, Ph.D. thesis, Cornell University, Ithaca, NY, 1997, in preparation.
[12] B. Thuillot, A. Goswami, and B. Espiau, in *Proc., 1997 IEEE International Conference on Robotics and Automation*, IEEE (IEEE, New York, NY, 1997), pp. 792–8.
[13] J. V. Fowble and A. D. Kuo, in *Biomechanics and Neural Control of Movement*, Engineering Foundation Conferences (EFC, Mount Sterling, OH, 1996), pp. 28–9.
[14] M. Coleman *et al.*, in press, Proc., IUTAM Chaos '97 Symposium (unpublished).
[15] R. S. Hand, Master's thesis, Cornell University, Ithaca, NY, 1988.
[16] J. Papadopoulos, private communication (unpublished).
[17] Y. Rocard, *General Dynamics of Vibrations*, 3rd ed. (Frederick Ungar Publishing Co., New York, 1960).
[18] R. S. Sharp, in *Proc., 8th IAVSD–Symposium; The Dynamics of Vehicles on Roads and Tracks*, IAVSD–IUTAM, edited by J. K. Hedrick (Swets and Zeitlinger B. V., Lisse, 1983), pp. 564–77.
[19] M. Hubbard, J. Appl. Mech. **46**, 931 (1979).
[20] T. Cardanha and R. Bennet, Cornell University Engineering Undergraduate Research Project (unpublished).
[21] A. Ruina, submitted to Reports on Mathematical Physics (unpublished).

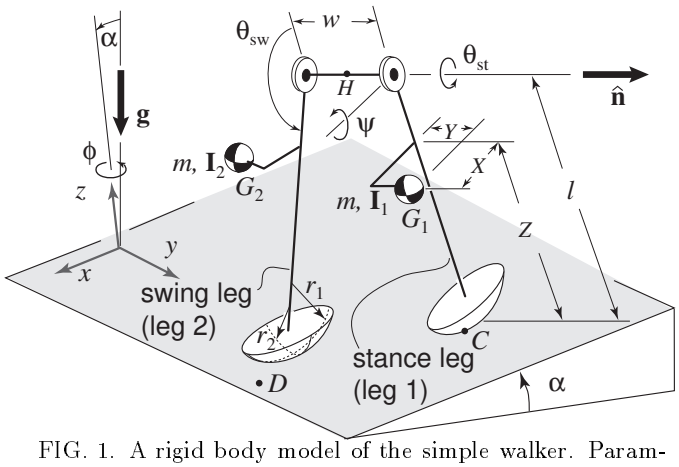

FIG. 1. A rigid body model of the simple walker. Parameters and state variables are described in the text.

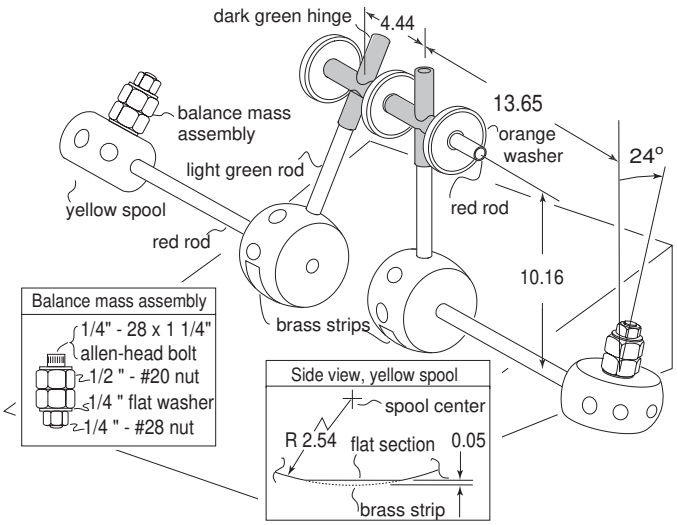

FIG. 2. The 3D Tinkertoy® walking model with hardware description and dimensions (in centimeters, not drawn to scale). The balance masses and the brass strips are fastened with black electrical tape (not shown).